RCMNS INTERIM COLLOQUIUM 2019

Continental-marine interactions during the Neogene in the Mediterranean area

Granada - Spain, 9-12 September 2019

FIELD GUIDE

UNIVERSIDAD DE GRANADA

Facultad de Ciencias

Departamento de Estratigrafía y Paleontología

From a marine embayment to a desiccated basin: the marine to continental transition in the Granada basin (Late Miocene, SE Spain). A field trip.

José M. Martín and Antonio García-Alix

Departamento de Estratigrafía y Paleontología. Universidad de Granada (Spain)

INTRODUCTION

In the Betic Cordillera, in southern Spain, a number of sedimentary basins differentiated during the Neogene, as a consequence of differential uplifting during the Alpine Orogeny. Some of these basins opened directly to the Mediterranean Sea, while others maintained links with the Atlantic Ocean through the Guadalquivir foreland basin (Braga et al. 2003) (Fig. 1). The connections between the Mediterranean-linked basins and the Atlantic-linked basins were limited to a few seaways that progressively closed in the course of the late Miocene (Martín et al. 2014).

Two different types of Mediterranean-linked basins can be distinguished: the *'inner basins'*, such as the Granada basin, located far from the present-day Mediterranean Sea, and the *'outer basins'*, such as the Sorbas basin, near to the present-day Mediterranean Sea (Braga et al. 2003) (Fig. 1). In the latest Tortonian-early Messinian, the *inner basins* were disconnected from the Mediterranean Sea and became continental, while the *outer basins* maintained their links, in some cases up to the Pliocene (Braga et al. 2003).

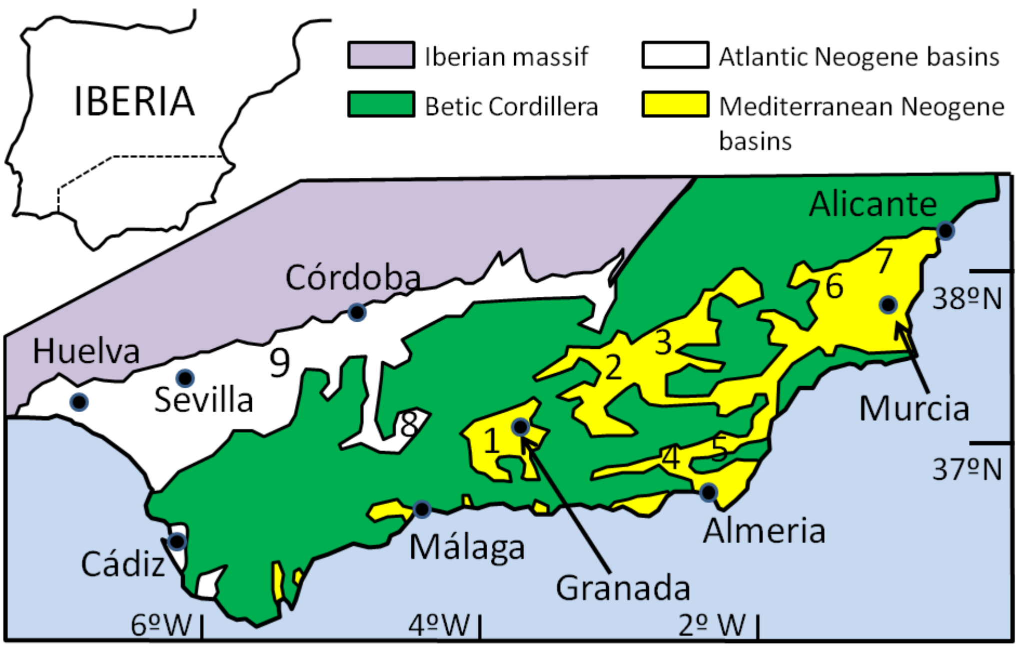

Figure 1. Main Mediterranean-linked and Atlantic-linked Neogene basins in the Betic Cordillera (1) Granada; (2) Guadix; (3) Baza; (4) Tabernas; (5) Sorbas; (6) Lorca; (7) Fortuna; (8) Ronda and (9) Guadalquivir basins (modified from Braga et al. 2003).

The Granada Basin is a small (50 x 50 km^2) Neogene intramontane basin located in the central part of the Betic Cordillera (Fig. 2). The basin's sedimentary infill unconformably overlies an irregular, fault-controlled, basement paleorelief (Morales et al. 1990), consisting of rocks from the Internal and the External Zones of the Cordillera. A series of sedimentary units can be differentiated in the Neogene-Quaternary infilling of the Granada basin (Braga et al. 1990, 2003) (Figs 2 and 3). Major fault systems have E-W orientations (Sanz de Galdeano 2008). Secondary faults, with a NW-SE trending, cut and displace the E-W faults and define the principal subsiding areas of the central and eastern part of the Granada Basin (Rodríguez-Fernández and Sanz de Galdeano 2006).

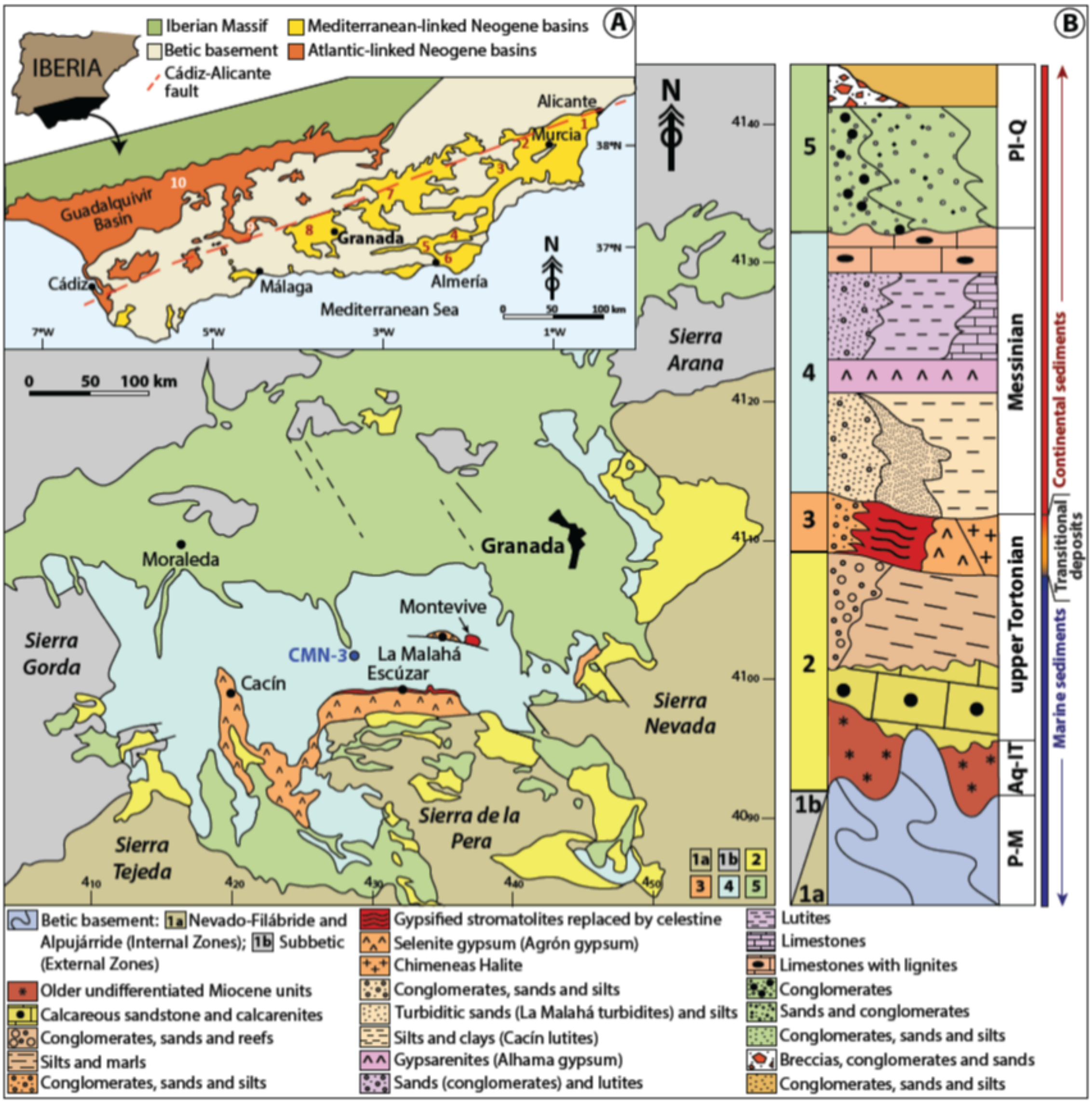

Figure 2 A. Inset showing the position of the Granada basin within the Betic Cordillera. **B:** Stratigraphic column and simplified geological map of the Granada basin (modified from Dabrio et al. 1982, and Martín et al. 1984).

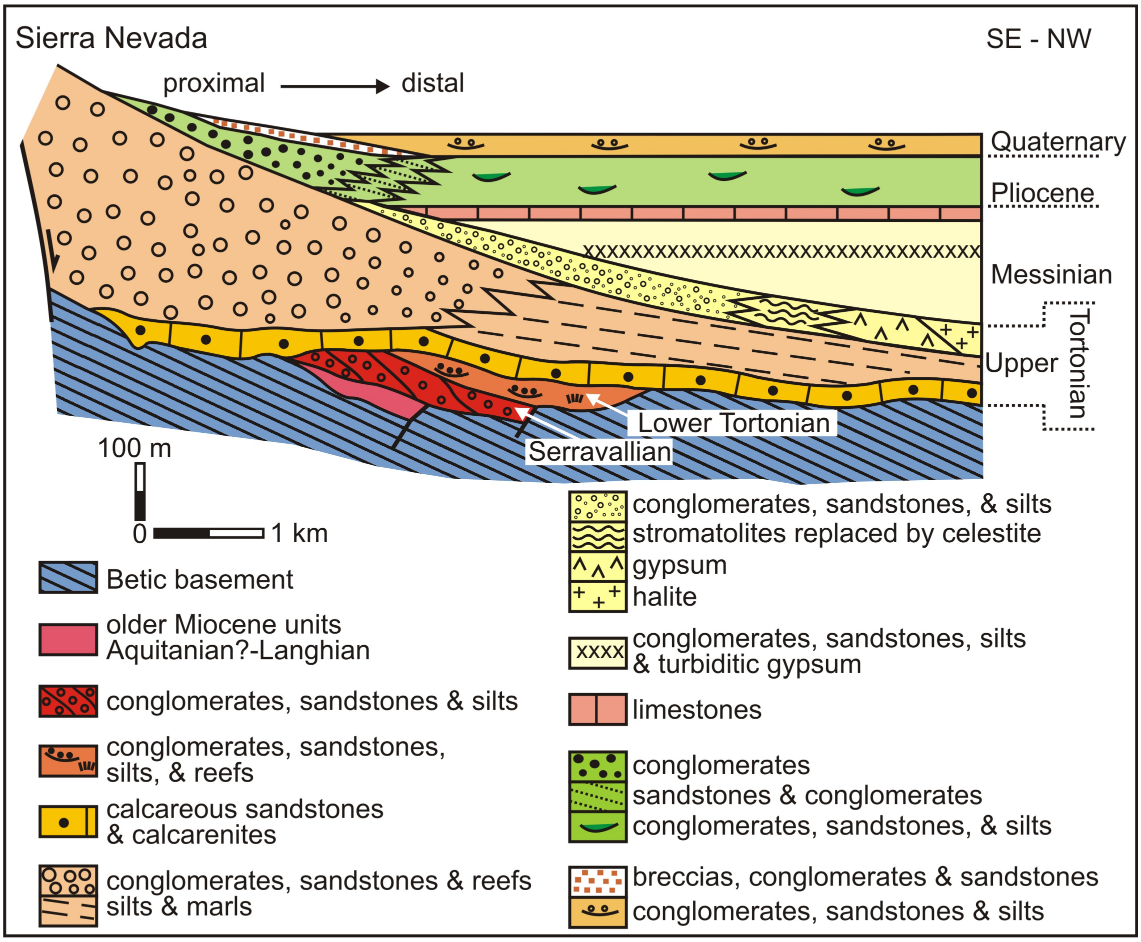

Figure 3. Stratigraphy of the Granada basin (from Braga et al. 2003).

The Granada Basin as such differentiated in the late Tortonian (Braga et al. 2003; Rodríguez-Fernández and Sanz de Galdeano 2006), at around 8.3 Ma (Corbí et al. 2012). At first it was a marine embayment, connected to the Atlantic Ocean and the Mediterranean Sea (Braga et al., 2003; Martín et al. 2014), and then only to the Mediterranean Sea (Braga et al. 1990) (Fig. 4). From 8.3 to 7.3 Ma, major tectonic activity took place in the northeastern (Sierra Arana) and eastern (Sierra Nevada) highland edges of the basin, resulting in the deposition of significant amounts of conglomerates at the base of the uplifted areas (Braga et al. 1990, 2003; Martín and Braga 1997) (Fig. 4). Skeletal carbonates accumulated in siliciclastic-free areas on platforms around the marine-basin margins. Temperate-water carbonates (Puga-Bernabéu et al. 2008; López-Quirós et al. 2016) formed first, between 8.3 and 7.8 Ma (Corbí et al. 2012), followed by tropical, coral-reef carbonates (Braga et al. 1990), between 7.8 and 7.3 Ma (Corbí et al. 2012). In the latest Tortonian (7.3 to 7.2 Ma, Corbí et al. 2012), due to a major regression resulting from a significant eustatic sea-level fall associated with local tectonic uplift, the Granada Basin desiccated (Martín et al. 1984) and became continental.

Figure 4. Reef development and palaeogeography of the Granada basin during the Upper Tortonian (~ 7.5 Ma ago) (from Braga et al. 1990).

The Granada Basin contains a thick, uppermost Tortonian evaporite succession (the 'Lower Evaporites' of Dabrio et al. 1982), formed under transitional marine to continental conditions (Martín et al. 1984). This Evaporite Sequence, from the margin to the center of the basin, has the following deposits (Fig. 5): a) stromatolites replaced by celestine (the 'Montevive and Escúzar Celestine') (Fig. 6); b) selenite gypsum (the 'Agrón Gypsum') (Fig. 7), and c) halite (the 'Chimeneas Halite') (Martín et al. 1984; García-Veigas et al. 2013, 2015) (Fig. 8). In the salt succession (up to 500 m thick), García-Veigas et al. (2013) identified three halite-bearing units: the 'Lower Halite Unit' (LHU), the 'Intermediate Sandstone Unit' (ISU) and the 'Upper Halite Unit' (UHU) Fig. 9). Isotope data and bromine content indicate a marine origin for the "Lower Halite", which formed in a shallow, marine lagoon (García-Veigas et al. 2013).

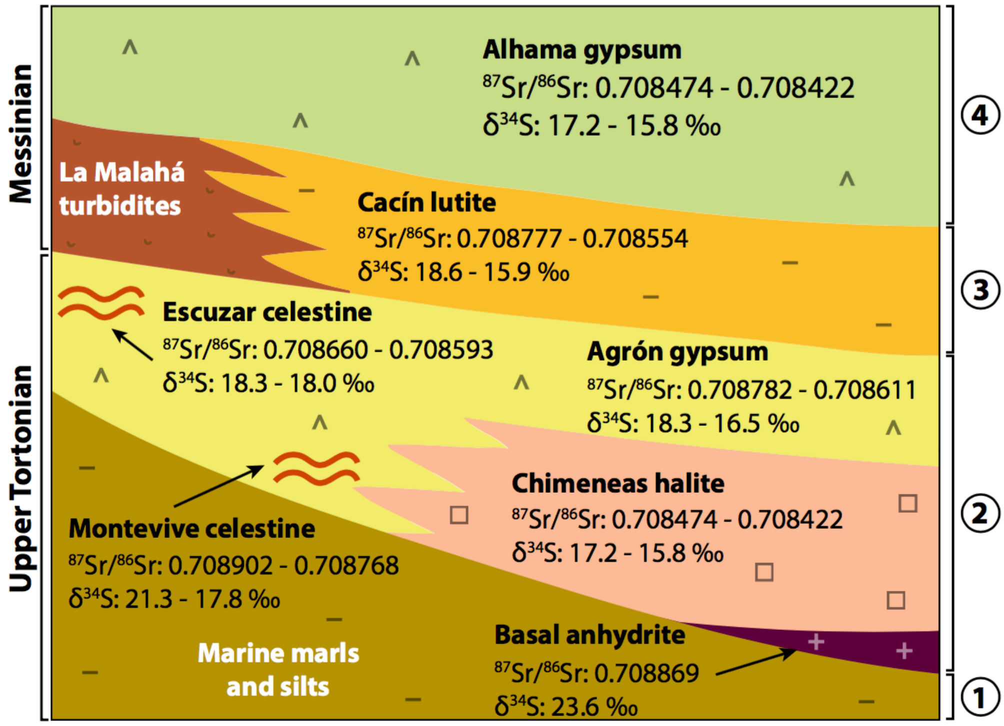

Figure 5. The "Lower Evaporites" (in the sense of Dabrio et al., 1982, and Martín et al., 1994, number 2 in the diagram) comprise the following deposits: "Montevive and Escúzar Celestine", "Agrón Gypsum" and "Chimeneas Halite", and formed at the time the Granada basin desiccated and became continental. $\delta^{34}S$ and $\delta^{18}O$ and $^{87}Sr/^{86}Sr$ data after García-Veigas et al. (2013, 2015).

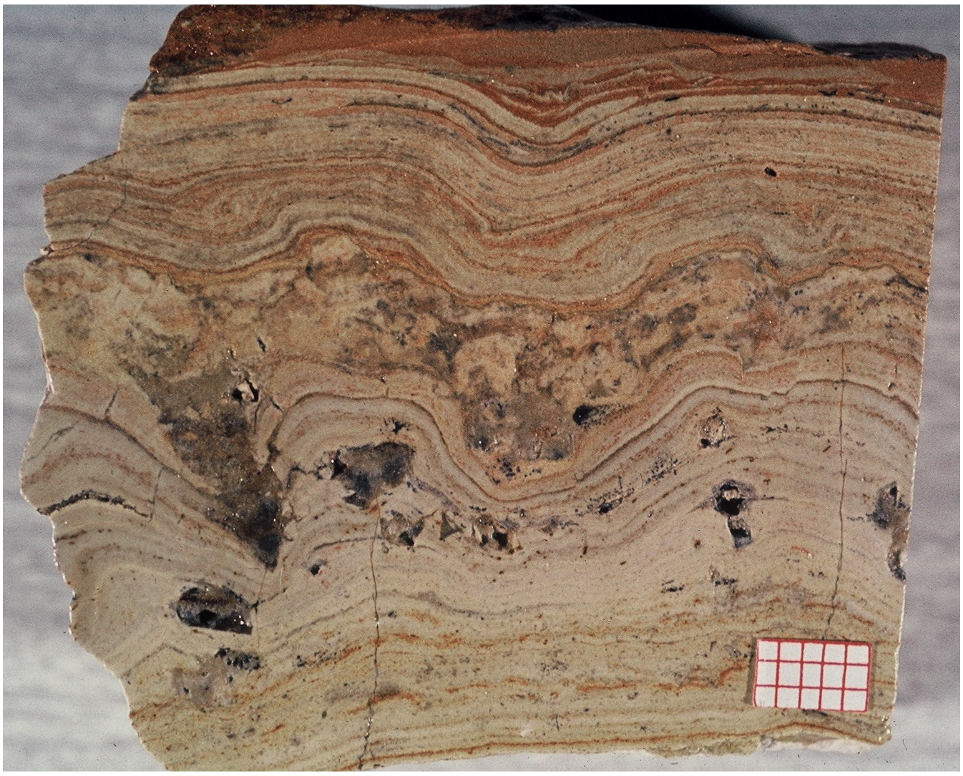

Figure 6. Stromatolite replaced by celestine. Montevive deposit (scale = 1 cm).

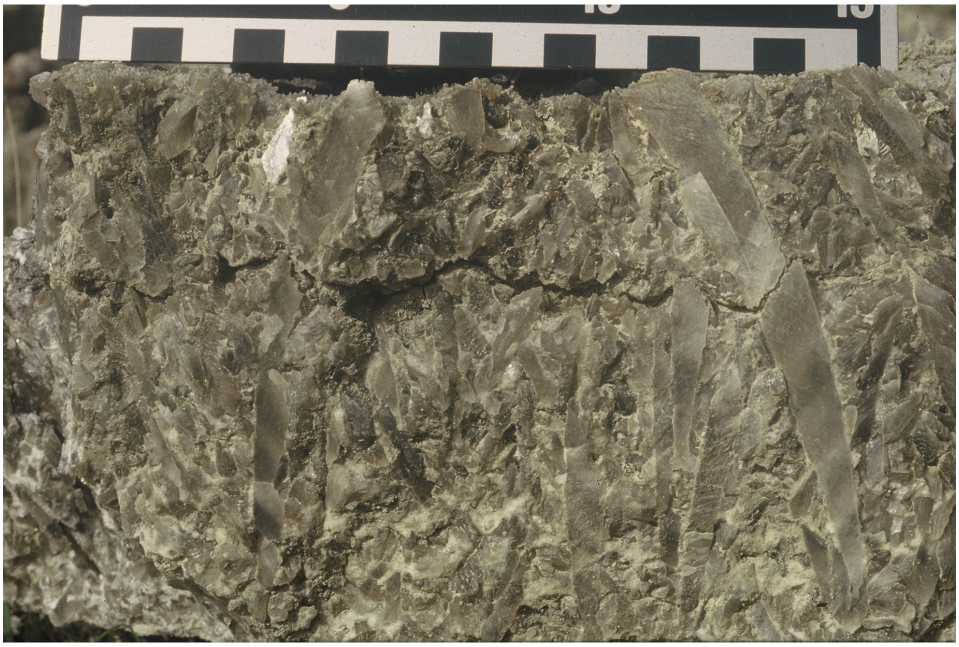

Figure 7. Selenite gypsum. Locality: Cacín (scale = 15 cm).

ISU deposits (Fig. 10) mark the first step in the growing influence of non-marine conditions in the Granada Basin. Sedimentological, petrological, and geochemical ($\delta^{34}S$ and $\delta^{18}O$ and $^{87}Sr/^{86}Sr$) data indicate that ISU deposition took place in a coastal lake, isolated from the open sea by a sand barrier (López-Quirós et al. 2018) (Fig. 11). Three main stages are recognized in the evolution of the lake (Fig. 12). At stage 1, syn-depositional anhydrite nodules formed close to the surface in a very shallow lacustrine environment. At Stage 2, frequent marine flooding storm events resulted in significant bioclastic sandy sedimentation in a presumably deeper lake. At Stage 3, a shallower, perennial saline lake was established and major evaporite deposition (anhydrite after micro-selenite gypsum, and primary chevron halite) took place. Isotope analyses point to a mixture of different inflow waters, including marine and underground (hydrothermal)-water inputs for the origin of the brines (López-Quirós et al. 2018) (Fig. 11).

During the Messinian (Fig. 13) and the Pliocene (Fig. 14), the continental Granada Basin was filled by detrital (alluvial-fan and fluvial) and carbonate/evaporite (lacustrine) deposits (Dabrio et al. 1982; Martín et al. 1984; Fernández et al. 1996; García-Alix et al. 2008; García-Veigas et al. 2015). During the Quaternary (Fig. 15), sedimentation concentrated in small, fault-controlled, high-subsidence depocentres (Morales et al. 1990; Rodríguez-Fernández and Sanz de Galdeano 2006; García-Alix et al. 2009), filled by detrital sediments (mostly conglomerates).

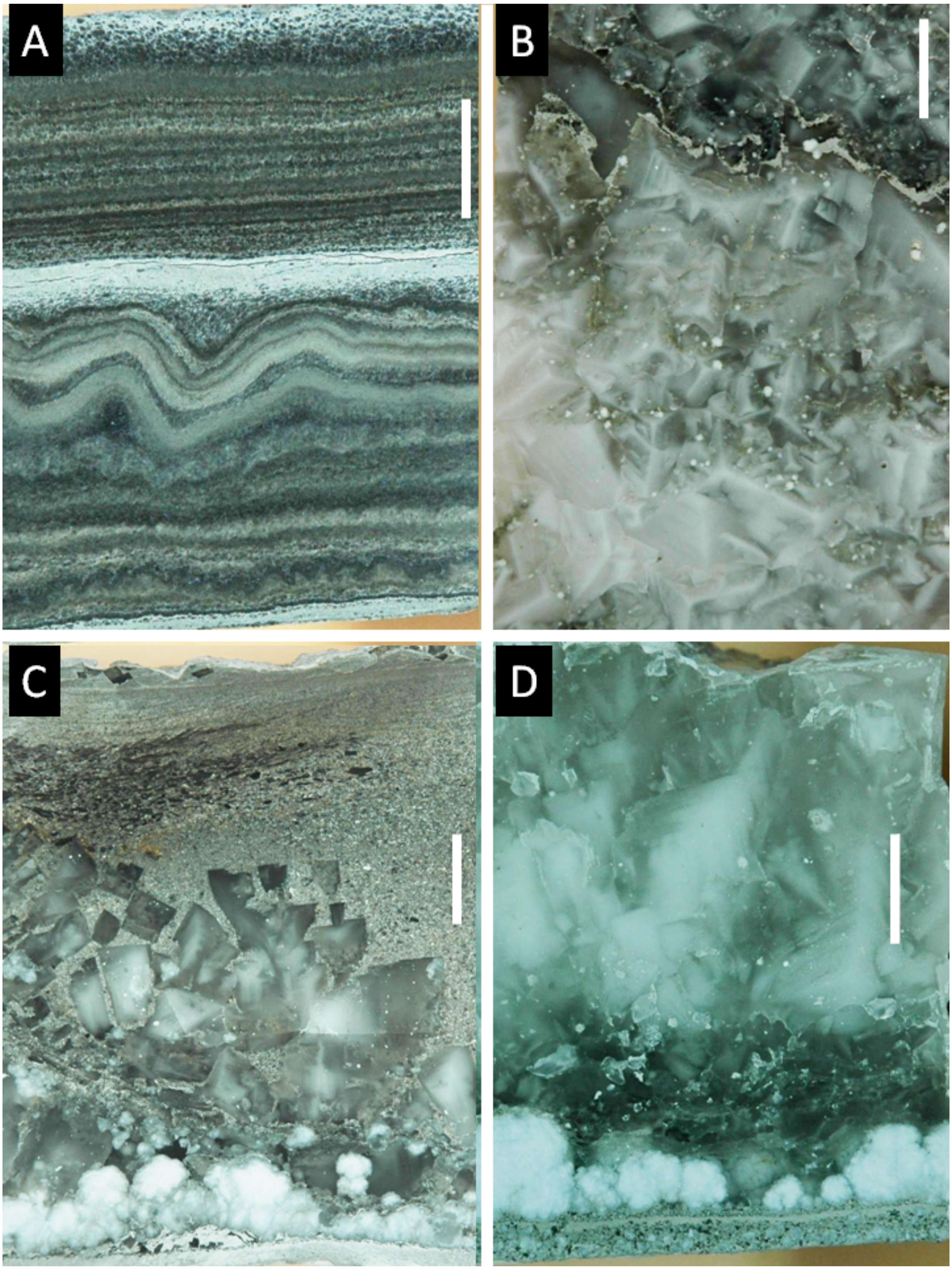

Figure 8. "Chimeneas Halite". A: Laminated, basal anhydrite bed. B: Poorly-bedded halite from the LHU. C: Chevron halite crystals from the ISU. D: Banded halite, with chevron halite crystals on top, from the UHU (scale bar = 1 cm).

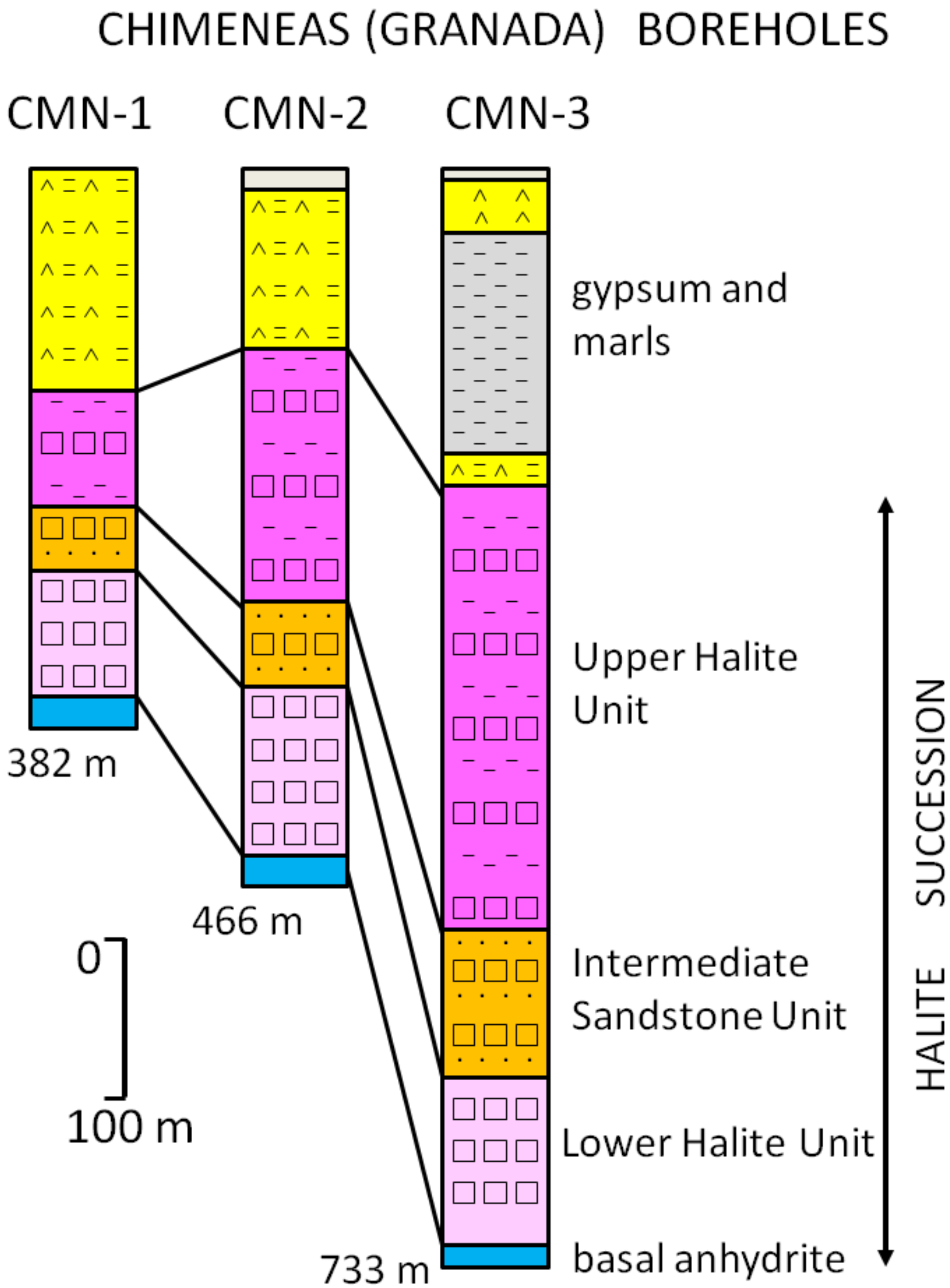

Figure 9. The halite succession, comprising three units, the "Lower Halite Unit" (LHU), the "Intermediate Sandstone Unit" (ISU) and the "Upper Halite Unit" (UHU), has been drilled in three holes near Chimeneas. Its maximum thickness, up to 500 m of salt, is reached at CNM-3 borehole (see Fig. 2 for location).

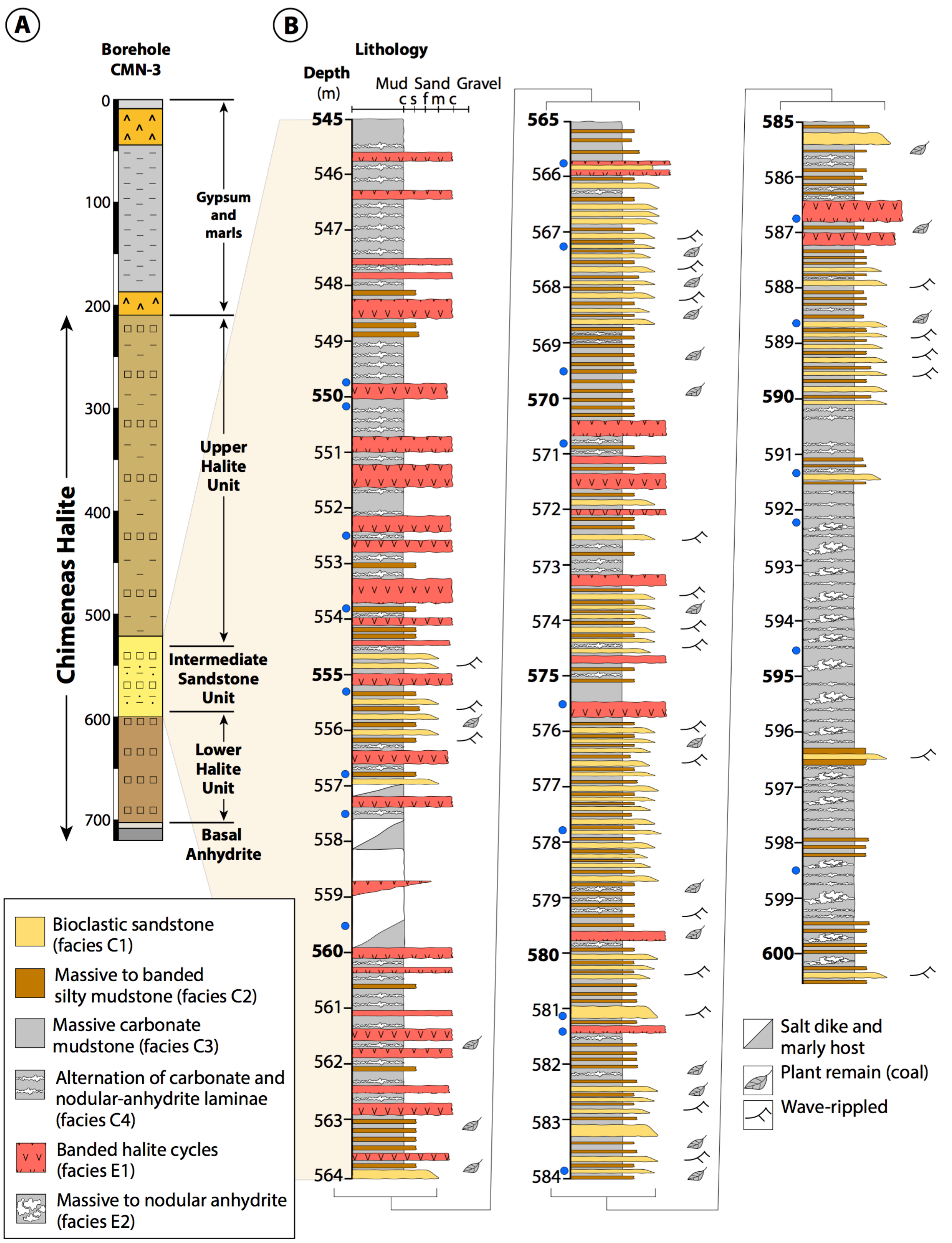

Figure 10. Detail log of ISU ("Intermediate Sandstone Unit") deposits at CNM-3 borehole (from López-Quirós et al. 2018).

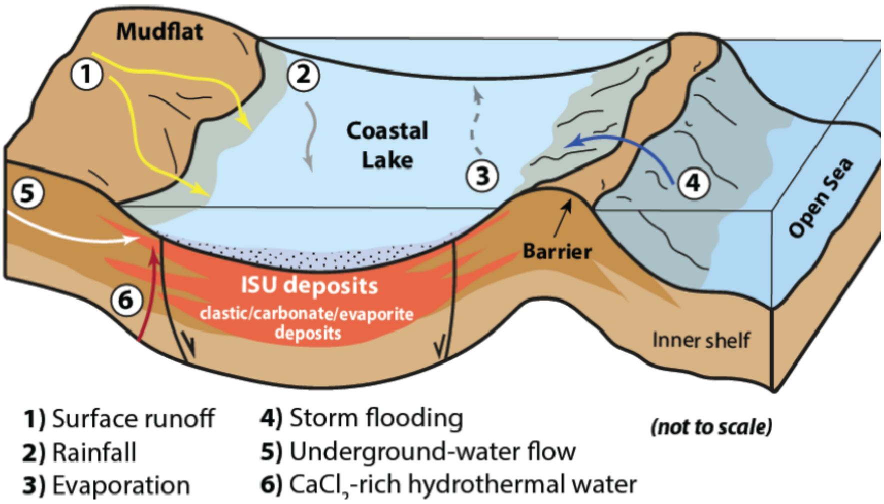

Figure 11. The depositional model for the halite-bearing, ISU ("Intermediate Sandstone Unit") deposits was that of a coastal lake, isolated from the open sea by a bioclastic, sandy barrier. Salt brines derived from a mixing of inflow waters coming from different sources, including marine and underground (hydrothermal) waters (from López-Quirós et al. 2018).

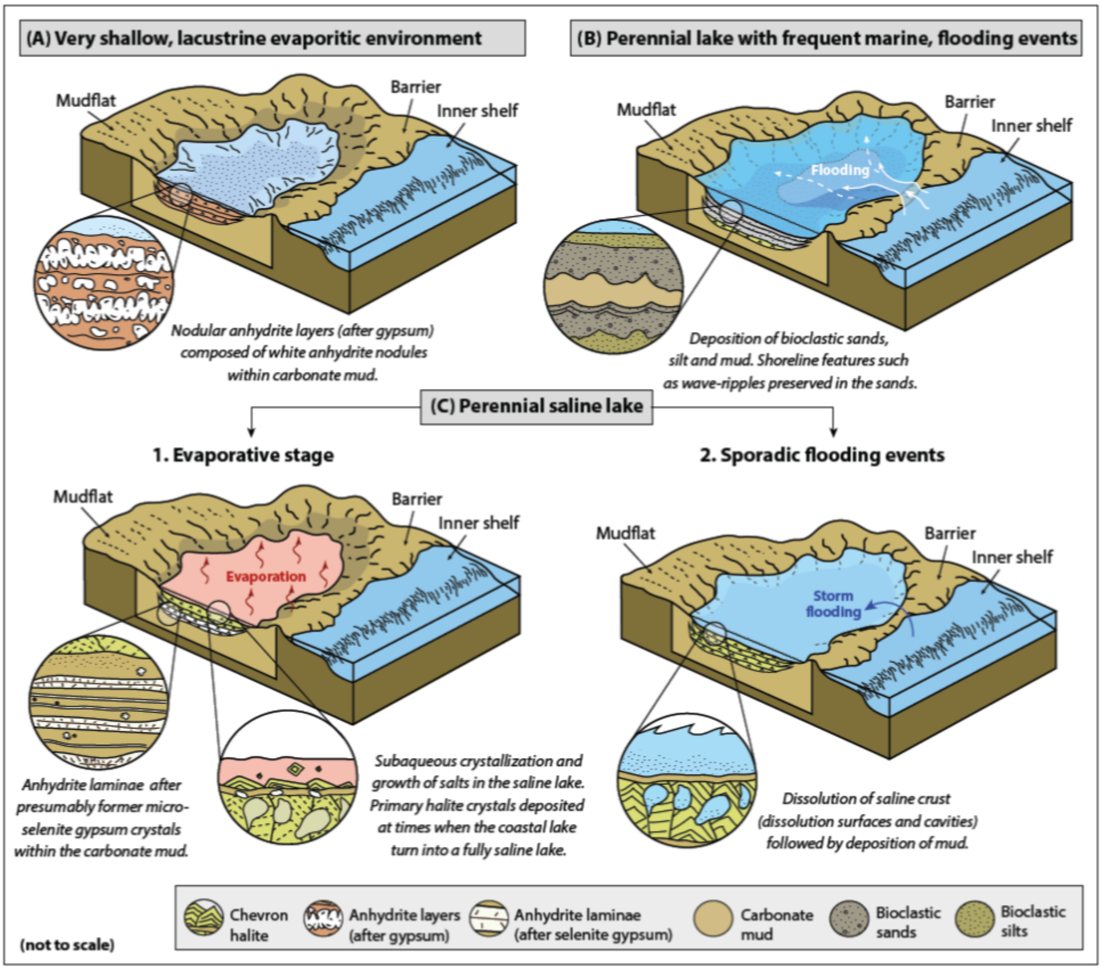

Figure 12. Stages of evolution of the ISU ("Intermediate Sandstone Unit") coastal lake and resulting deposits (from López-Quirós et al. 2018).

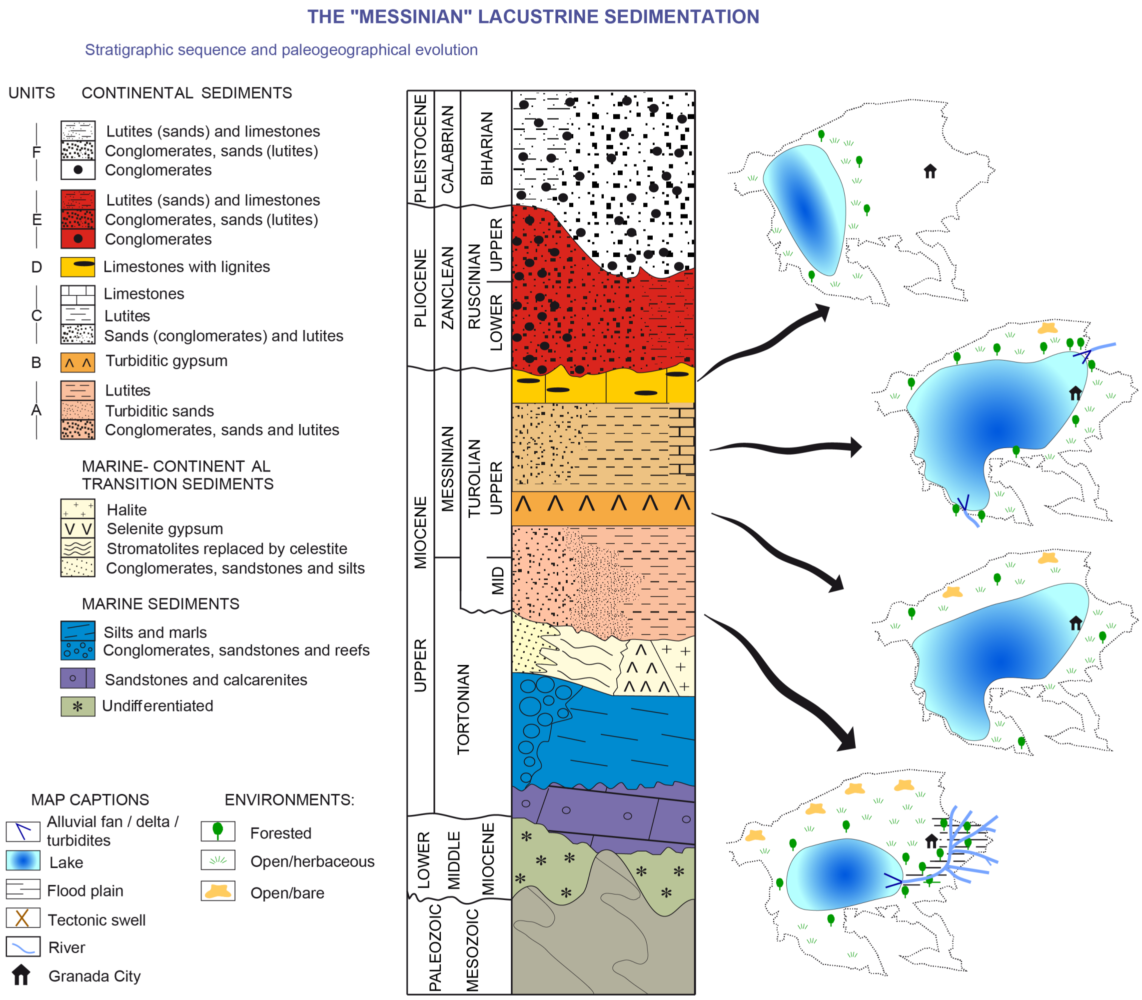

Figure 13. Stages of evolution of the "Messinian" (Turolian) lake in the Granada Basin and resulting deposits (from García-Alix et al. 2008).

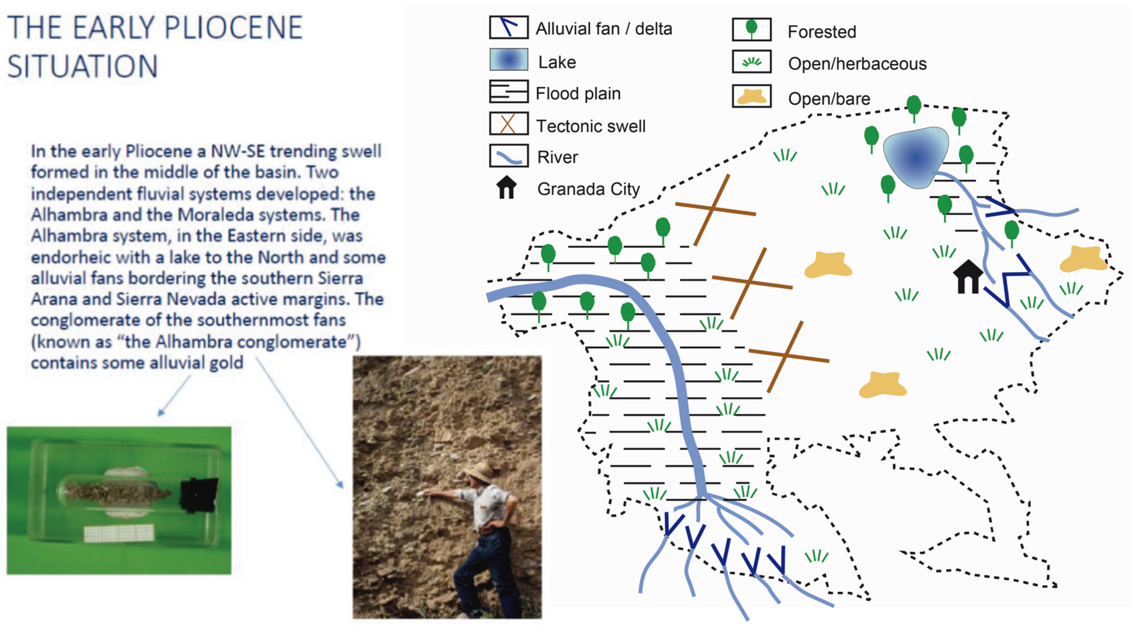

Figure 14. Two independent fluvial systems developed in the Granada basin during the Pliocene: the "Alhambra" and the "Moraleda" systems, separated by a tectonic swell, trending NW-SE and located in the middle of the basin (from García-Alix et al. 2008).

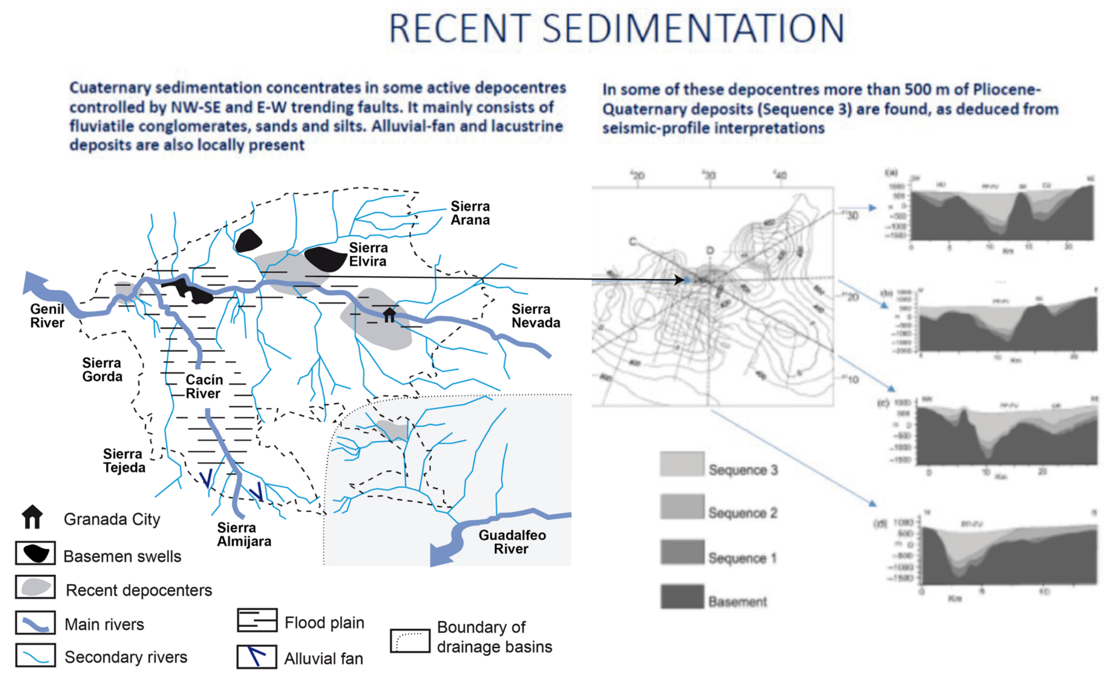

Figure 15. Quaternary sedimentation in the Granada basin concentrates in some active depocentres controlled by NW-SE and E-W trending faults (from Rodríguez-Fernández and Sanz de Galdeano 2006, and García-Alix et al. 2009).

DESCRIPTION OF THE FIELD STOPS

Location of the field stops. Red dots show the approximate boundary of the Granada Basin.

First stop: The Alhama-river canyon.

Sediments from the first marine Upper Tortonian unit (locally known as "Maciños"), aged between 8.3 and 7.8 (Corbí et al. 2012), are well exposed along the vertical walls of the Alhama-river canyon (Fig. 16). They were deposited in a small bay located at the southwestern margin of the Granada basin (Fig. 17). They consist of bioclastic sands at the base (Fernández and Rodriguez-Fernández, 1991), crowned by carbonates on top (Puga-Bernabéu et al. 2008). Bioclastic sands, up to 35 m thick, exhibit frequent herringbone cross stratification (Fig. 18) attesting for tidal action, and scape burrows (Fig. 19). The carbonates, up to 45 m thick, are bioclastic calcarenites and fine-grained calcirudites containing abundant and highly fragmented skeletal remains of bivalves, bryozoans and coralline algae, a bioclastic association very common in temperate-water carbonates. The depositional model for the carbonates is shown on Fig. 20A (Puga-Bernabéu et al. 2008). Low-angle, parallel-laminated bioclastic sediments accumulated at the beach. At a small distance from the coast, at shallow depths, a shoal system developed, with small bars, moved by waves, close to the shore line, and large sandwaves (Fig. 21), moved by longshore currents, developed more to seawards. The so-called "factory-zone", where most of the bioclast-producing organisms lived and proliferated, occurred at a greater depth, within the platform. Most conspicuous sedimentary structures in the carbonates are trough cross-bedding and horizontal, parallel-lamination (Fig. 22), attesting for wave and storm action respectively (Fig. 20B). *Scolicia* burrows are frequently found (Fig. 23).

Figure 16. The Alhama river canyon.

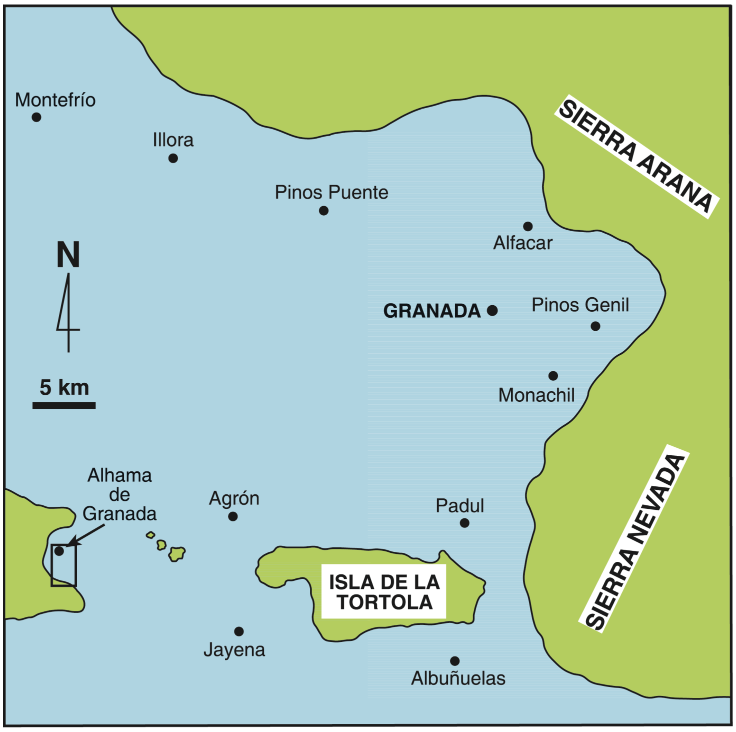

Figure 17. Palaeogeography of the Granada basin at the time of deposition of the "Maciños" Unit (~ 8 Ma): a large embayment, connected both to the Atlantic Ocean to the NW and to the Mediterranean Sea to the S-SW, and then only opened to the Mediterranean Sea. The Alhama outcrop locates at the south-westernmost margin of the basin (from Puga-Bernabéu et al. 2008).

Figure 18. Bioclastic sands exhibiting, metre-scale herringbone cross-stratification.

Figure 19. Scape burrows in bioclastic sands.

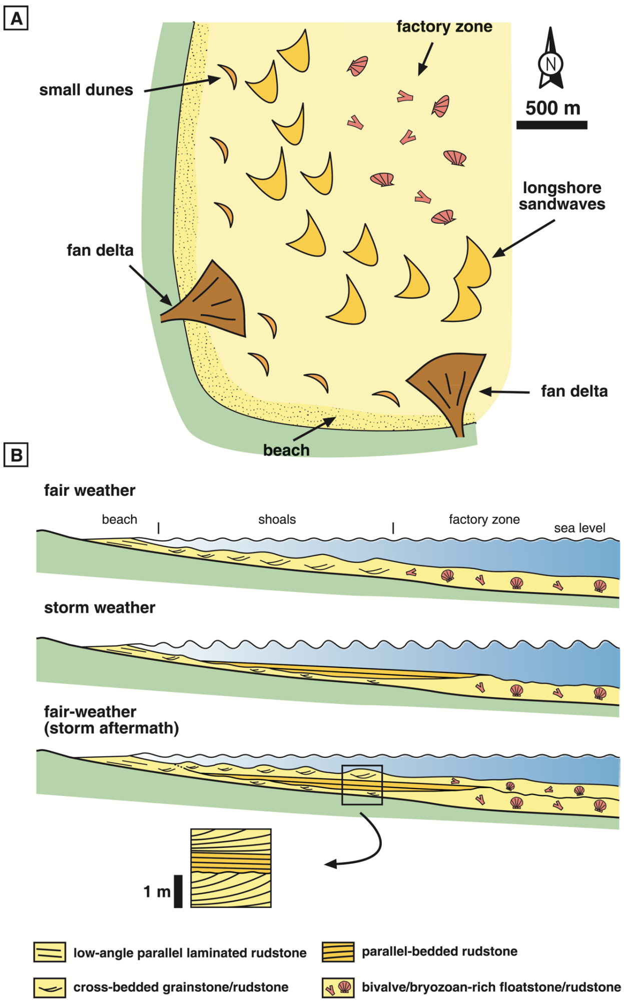

Figure 20. A: Depositional model for the "Alhama carbonates". **B:** A combination between fair-weather episodes and storm-related events generated the trough cross-bedded/horizontal, parallel-laminated stratum-alternation (from Puga-Bernabéu et al. 2008).

Figure 21. “Alhama carbonates”. Cross-bedded strata of a large sand-wave, presumably moved by longshore currents, stand out in the middle of the picture.

Figure 22. “Alhama carbonates”. Alternation between trough cross-bedded and horizontal, parallel-laminated strata. Cross and parallel lamination is locally disturbed by *Scolicia* burrows.

Figure 23. “Alhama carbonates”. *Scolicia* burrows seen in close view.

Figure 24. “Alhama carbonates”. Submarine-canyon infilling-sediments unconformably overlying and cross cutting older carbonate-platform strata.

An outstanding feature in the carbonates is the existence of a former submarine canyon. Canyon-infilling sediments unconformably overlie and cross cut the platform carbonate strata (Fig. 24). Sediment infilling of the canyon occurred by collapsing of longshore bars and by storm mobilization and redeposition, of bioclastic sediment cascading from the top of the canyon walls (Puga-Bernabéu et al. 2008) (Fig. 25).

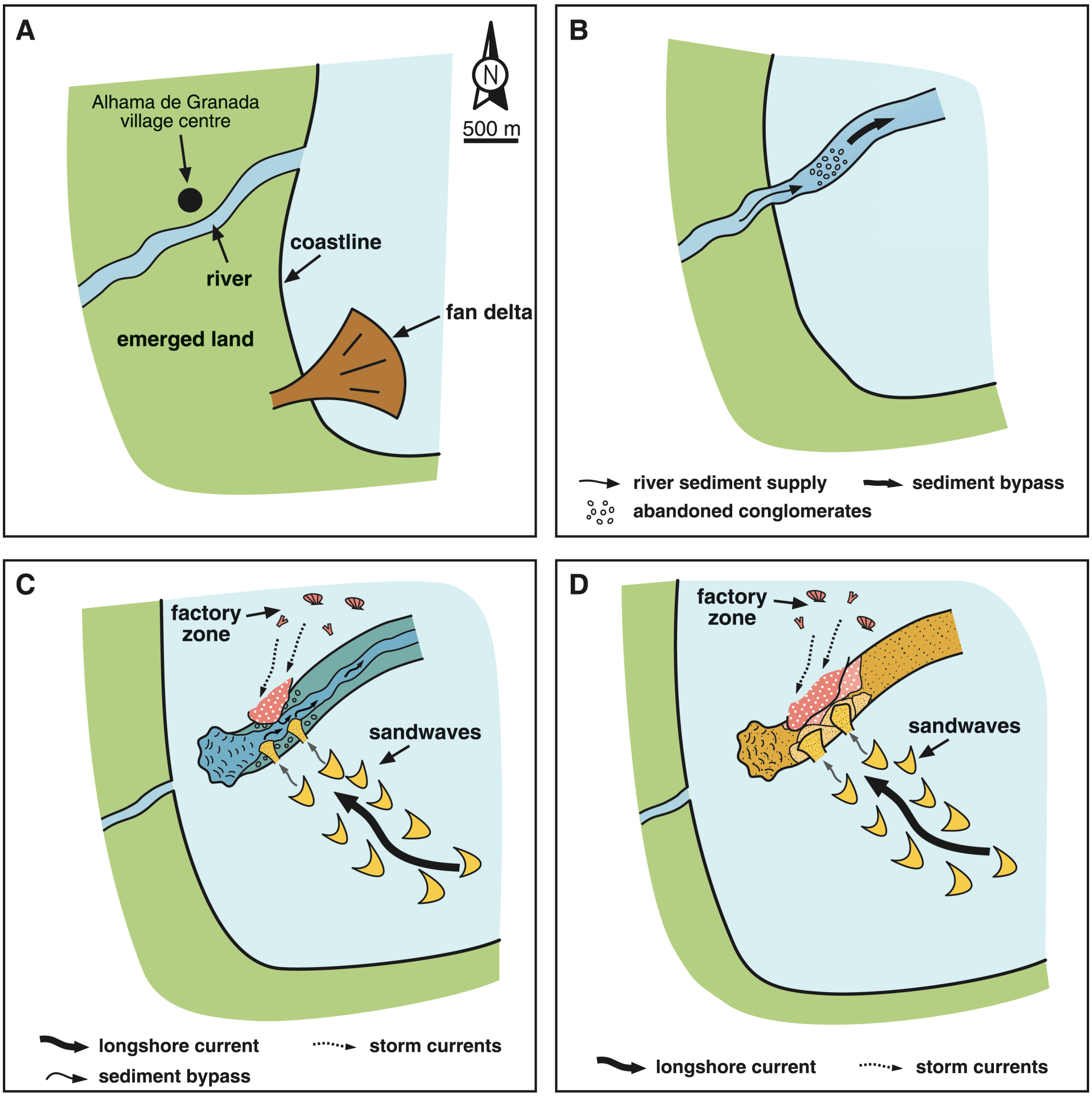

Figure 25. A-D: Stages of evolution and infilling of the "Alhama submarine canyon" (from Puga-Bernabéu et al. 2008).

Second stop: The Ventas de Huelma gypsum quarry.

The "Agrón Gypsum" is well exposed in an abandoned quarry near Ventas de Huelma. Single gypsum layers, up to 30 cm thick, are made up of alabaster gypsum and are separated by fine (mm to a few cm thick) marl "seams" (Fig. 26). This gypsum unit may reach up to 200 m in thickness in close, nearby areas. This variety of gypsum resulted from secondary (diagenetic) alteration of primary gypsum, and transformation via anhydrite, after burial. Primary selenite layers, sometimes accompanied by balatino (primary, fine-grained) gypsum, are only found at the westernmost part of the quarry (Fig. 27).

Figure 26. Well-stratified, alabaster-gypsum layers are superbly exposed at the abandoned Ventas de Huelma gypsum quarry.

Figure 27. Ventas de Huelma gypsum quarry. Primary selenite gypsum is only found at the westernmost corner of the quarry.

Third stop: The La Malahá vantage point.

From the top of a nearby hill, just North of the La Malahá village, there is magnificent view of the area where most of the "Lower Evaporites", including the thick salt deposits, accumulated (Fig. 28A-B). Sediments from the lowermost "Messinian" (Middle-Upper Turolian) lacustrine unit (García-Alix et al. 2008) (unit A in Fig. 13) outcrop here. They consist of turbidite sands (the "La Malahá turbidites "of Dabrio et al. 1972) changing laterally to, and interfingering with, finely-laminated silts (the "Cacin lutites" of Dabrio et al. 1972, 1982). The southern boundary of the hill is lined by a fault system, the "La Malahá fault system", active since the Late Tortonian and, presumably, from earlier times. Note that the "La Malahá fault system" is the one separating the two major Basement Zones, and is also the one controlling the salt depocentre (Fig. 28C).

Looking at the SW, the basement outcrops of the Sierra de la Pera (also known as Sierra de la Tórtola) stand out in the middle ground, and those of the Sierra Tejeda at the background, in the distance (Fig. 29). A major uplifting pulse, which resulted in the emersion of the Sierra Tejada in the Latemost Tortonian, is thought to have been responsible for the subsequent isolation of the Granada basin from the Mediterranean Sea, leading to its desiccation. At the foot of hill, at the northern edge of the La Malahá village, a present-day "salina" (solar salt pond), worked since Roman times, is clearly visible (Figs 29 and 30). The very existence of this solar salt pond evidences the presence of a close, underground halite deposit from which the salt is being mobilized.

Two different types of underground-water springs are found at La Malahá: the hot-water spring of "Los Baños" (Roman Thermal Baths) and the saline spring feeding the "salina". They both are related to the "La Malahá fault system" and occur very close to each other, at a very short distance (Rosino, 2008) (Fig. 28C). Underground waters in both cases flow to the surface along some of the faults of the "La Malahá fault system". The underground water feeding the thermal spring comes from a deeper aquifer than that of the "salina" (Rosino, 2008).

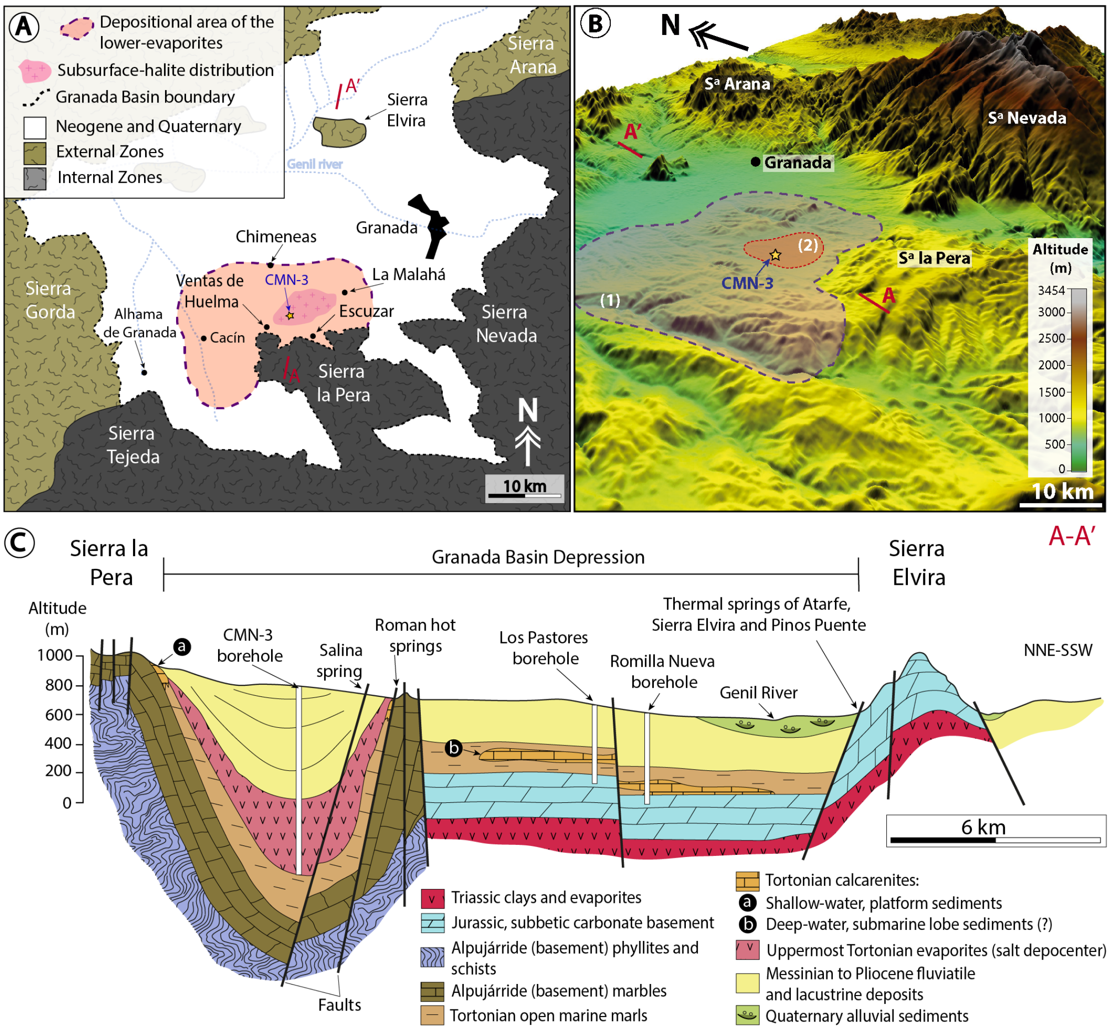

Figure 28. A and B: "Lower evaporite" depositional area. The precise positions of the halite deposits in the subsurface, the CNM-3 borehole, and the A-A´ cross-section (shown in Fig. 28C) are indicated (from López-Quirós et al. 2018). C: North-South cross-section of the Granada basin. The "La Malahá fault system" separates the two major Basement Zones and also controls the salt depocentre ((from López-Quirós et al. 2018; modified from Rosino, 2008).

Figure 29. The view to the SW shows at the far distance, behind the Sierra de la Pera in the mid-ground, the Sierra Tejeda. The uplifting and emersion of Sierra Tejeda in the Latemost Tortonian (~ 7.3 Ma) was responsible for the Granada basin isolation from the Mediterranean Sea, and its subsequent desiccation.

Figure 30. The "salina" (solar salt pond) of La Malahá. The Roman Tower, seen at the upper right-hand of the picture, is very close to the point where the saline-water spring locates. The saline water, which pours into the "Río Salado" river, is then pumped into the "salina", placed a couple of metres higher than the river bed.

Facing East, the Montevive celestine deposit (Martin et al. 1984; García-Veigas et al. 2015) is perfectly seen in the mid-ground (Fig. 31). This huge (1 Km long, 0'5 Km wide and 80 m thick) stromatolite buildup, heavily replaced by celestine, has been intensely mined at times since the mid-sixties in the last century. Stromatolites formed at the margin of the evaporite basin, coeval to the selenite gypsum and the halite basinal deposits (Martín et al. 1984; García-Veigas et al. 2015). Stromatolite replacement by celestine was a syn-sedimentary process, but the precise mechanism of replacement and the source for the strontium is still a matter of discussion (Martín et al., 1984; García-Veigas et al., 2015).

Figure 31. The Montevive Celestine deposit seen from the distance, with the Sierra Nevada behind, at the background.

References

Braga, J.C., Martín, J.M., Alcalá, B., 1990. Coral reefs in coarse-terrigenous sedimentary environments (Upper Tortonian, Granada Basin, southern Spain). Sedimentary Geology 66, 135–150.

Braga, J.C., Martín, J.M., Quesada, C., 2003. Patterns and average rates of late Neogene-Recent uplift of the Betic Cordillera, SE Spain. Geomorphology 50, 3–26.

Corbí, H., Lancis, C., García-García, F., Pina, J.A., Soria, J.M., Tent-Manclús, J.E., Viseras, C., 2012. Updating the marine biostratigraphy of the Granada Basin (central Betic Cordillera). Insight for the Late Miocene palaeogeographic evolution of the Atlantic-Mediterraneas seaway. Geobios 45, 249–263.

Dabrio, C.J., García-Yebra, R., González Donoso, J.M., Vera, J.A., 1972. Turbiditas asociadas a evaporitas (Mioceno, La Malá, Depresión de Granada). Cuadernos de Geología 3, 139–164

Dabrio, C.J., Martín, J.M., Megias, A., 1982. Signification sédimentaire des évaporites de la depression de Granade (Espagne). Bulletin de la Societe Geologique de France 24, 705–710.

Fernández, J., Rodríguez-Fernández, J., 1991. Facies evolution of nearshore marine clastic deposits during the Tortonian transgression-Granada Basin, Betic Cordilleras, Spain. Sedimentary Geology, 71, 5–21.

Fernández, J., Soria, J., Viseras, C., 1996. Stratigraphic architecture of the Neogene basins in the central sector of the Betic Cordillera (Spain); tectonic control and base level changes. In: Friend, P.F., Dabrio, C.J. (Eds.), Tertiary Basins of Spain: The stratigraphic record of crustal kinematics. Cambridge University Press, Cambridge, UK, 353–365.

García-Alix, A., Minwer-Barakat, R., Martín, J.M., Martín-Suarez, E., Freudenthal, M., 2008. Biostratigraphy and sedimentary evolution of Late Miocene and Pliocene continental deposits of the Granada Basin (southern Spain). Lethaia 41, 431–446.

García-Alix, A. Minwer-Barakat, R., Martín, J.M., Martín-Suarez, E., Freudenthal, M., 2009. Dating the change from endorheic to exorheic conditions in the drainage system of the Granada basin (Southern Spain). Palaios 24, 544-549.

García-Veigas, J., Cendón, D.I., Rosell, L., Ortí, F., Torres Ruiz, J., Martín, J.M., Sanz, E., 2013. Salt deposition and brine evolution in the Granada Basin (Late Tortonian, SE Spain). Palaeogeography, Palaeoclimatology, Palaeoecology 369, 452–465.

García-Veigas, J., Rosell, L., Cendón, D.I., Gibert, L., Martín, J.M., Torres Ruiz, J., Ortí, F., 2015. Large celestine orebodies formed by early-diagenetic replacement of gypsified stromatolites (upper Miocene, Montevive-Escúzar deposits, Granada basin, Spain). Ore Geology Reviews 64, 187–199.

López-Quirós, A., Barbier, M., Martín, J.M., Puga-Bernabéu, Á. Guichet, X., 2016. Diagenetic evolution of Tortonian temperate carbonates close to evaporites in the Granada Basin (SE Spain). Sedimentary Geology 335, 180–196.

López-Quirós, A., Barbier, M., Martín, J.M., Guichet, X., 2018. Sedimentology and diagenetic evolution of the Neogene "Intermediate Sandstone Unit" in the halite deposits of the Granada basin (SE Spain): the turning point in the change from marine to continental sedimentation. Journal of Iberian Geology 44, 513-537.

Martín, J.M., Braga, J.C., 1997. Sierra Nevada: Historia del levantamiento de un relieve deducida de las unidades conglomeráticas de su borde. In: Calvo, J.P., Morales, J. (Eds.), Avances en el conocimiento del Terciario Ibérico. Grupo Español del Terciario, pp. 117–120.

Martín, J.M., Ortega-Huertas, M., Torres-Ruiz, J., 1984. Genesis and evolution of strontium deposits of the Granada Basin (southeastern Spain): evidence of diagenetic replacement of a stromatolite belt. Sedimentary Geology 39, 281–298.

Martín, J.M., Puga-Bernabéu, A., Aguirre, J., Braga, J.C., 2014. Miocene Atlantic-Mediterranean seaways in the Betic Codillera (southern Spain). Revista de la Sociedad Geológica de España 27 (1), 175–186.

Morales, J., Vidal, F., de Miguel, D., Aguacil, G., Posadas, A.M., Ibáñez, J.M., Guzmán, A., Guirao, J.M., 1990. Basement structure of the Granada Basin, Betic Cordilleras, southern Spain. Tectonophysics 177, 337–348.

Puga-Bernabéu, Á., Martín, J.M., Braga, J.C., 2008. Sedimentary processes in a submarine canyon excavated into a temperate- carbonate ramp (Granada basin, S. Spain). Sedimentology 55, 1449–1466.

Rodríguez-Fernández, J., Sanz de Galdeano, C., 2006. Late orogenic intramontane basin development: the Granada basin, Betics (southern Spain). Basin Research 18, 85–102.

Rosino, J., 2008. Modelo hidrogeológico conceptual de las aguas termo- minerales de la Depresión de Granada. En: J. A. López-Geta et al. (Eds.), Agua y Cultura. VII Simposio sobre el Agua en Andalucía (SIAGA-08), IGME, pp. 1107–1118.

Sanz de Galdeano, C., 2008. The Cádiz-Alicante fault: an important discontinuity in the Betic Cordillera. Revista de la Sociedad Geológica de España 21, 49–58.